

Supplementary Materials

Structure of mycobacterial maltokinase, the missing link in the essential GlgE-pathway

Joana Fraga^{a*}, Ana Maranha^{b*}, Vitor Mendes^b, Pedro José Barbosa Pereira^a, Nuno Empadinhas^b, Sandra Macedo-Ribeiro^a

^a IBMC – Instituto de Biologia Molecular e Celular, Universidade do Porto, Porto, Portugal

^b CNC - Center for Neuroscience and Cell Biology, University of Coimbra, Coimbra, Portugal

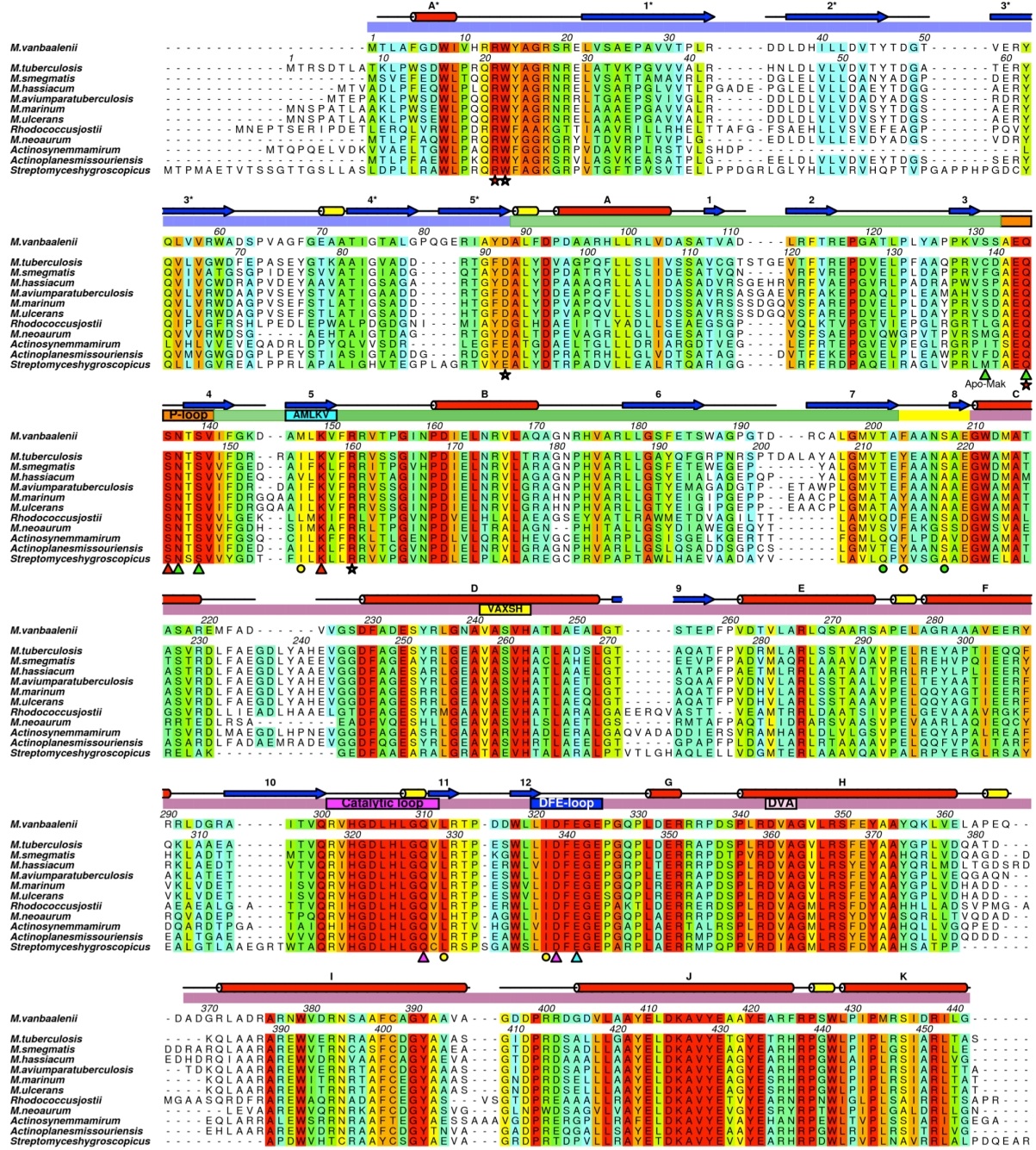
* - These authors contributed equally to this work and share first authorship.

Correspondence should be addressed to: Nuno Empadinhas (numenius@cnc.uc.pt) or Sandra Macedo-Ribeiro (sribeiro@ibmc.up.pt)

Supplementary Methods

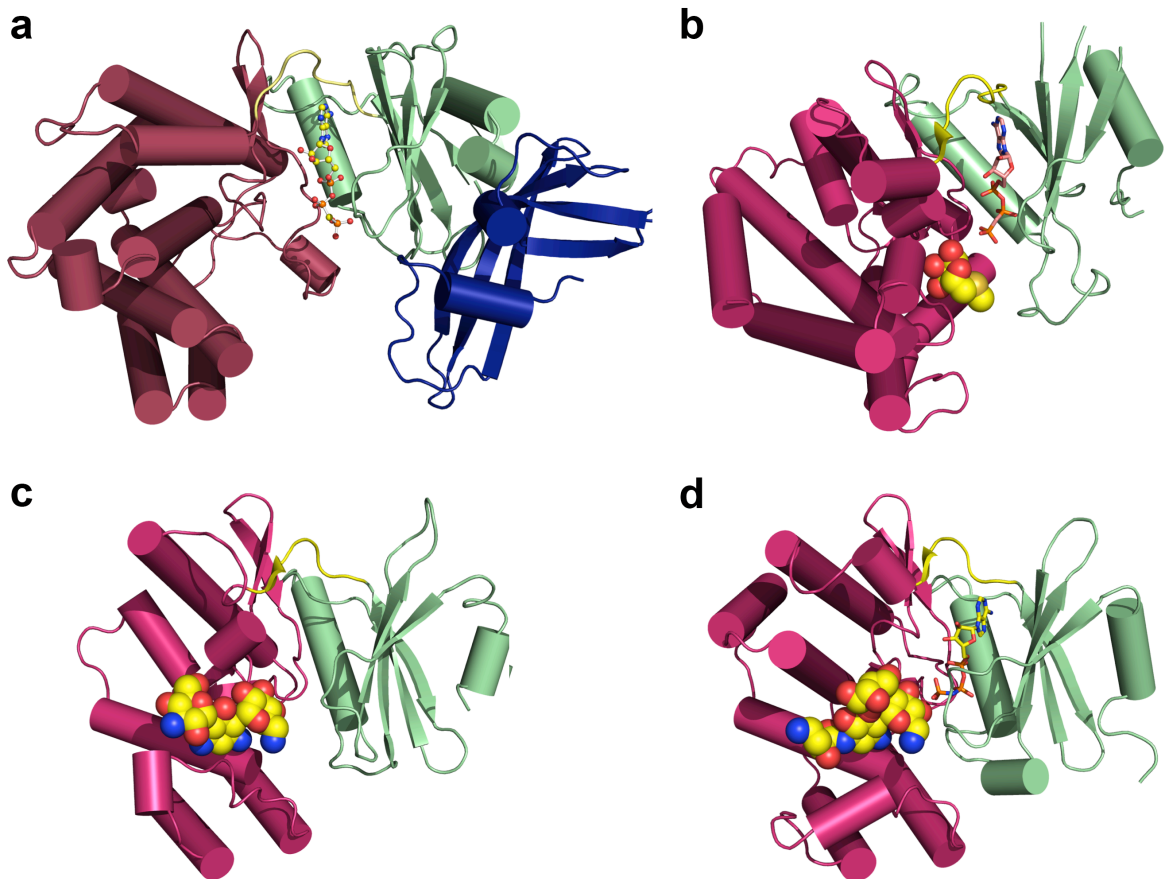
Circular dichroism measurements

The secondary structure of Mak^{Mvan}, Mak^{Mtb} and selected point mutants was determined by far-UV CD. Measurements of samples (0.1 mg/mL in 50mM BTP pH 7.5, 50 mM NaCl) were performed at 20°C on a Jasco J-815 spectrometer set up to 1 nm bandwidth, 1 s response, 200 nm/min scanning speed and 10 accumulations. Data were analysed and deconvoluted using the DichroWeb web server¹.



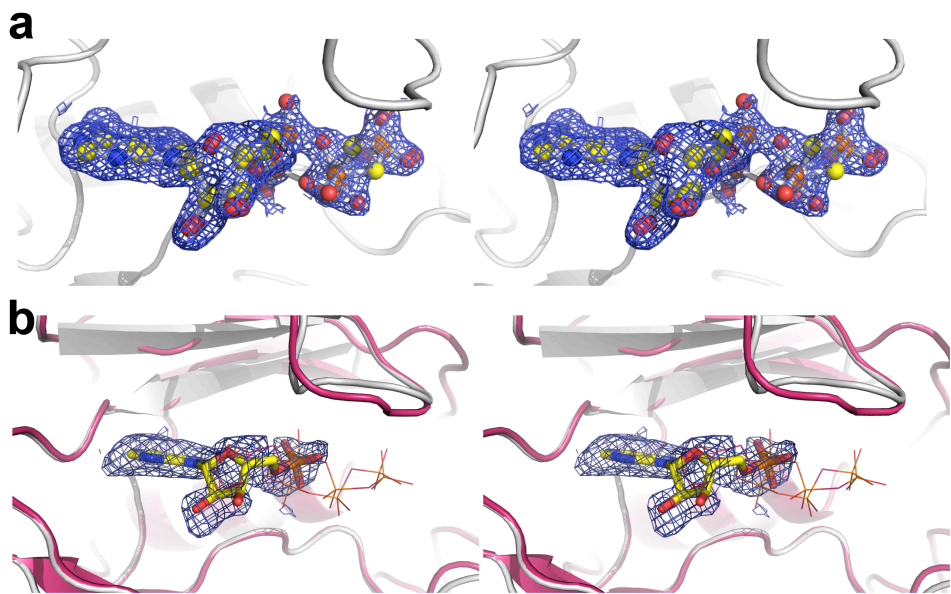
M. vanbaalenii 1 10 20 30 40 50 60
M. tuberculosis 1 MTRSDTLA 10 TKL PWS 20 WLR PQRWY 30 AGRNRELA 40 LAVKPGV 50 VVALR 60
M. smegmatis 1 MTRSDTLA 10 TKL PWS 20 WLR PQRWY 30 AGRNRELA 40 LAVKPGV 50 VVALR 60
M. haissiacum 1 MTRSDTLA 10 TKL PWS 20 WLR PQRWY 30 AGRNRELA 40 LAVKPGV 50 VVALR 60
M. aviumparatuberculosis 1 MTRSDTLA 10 TKL PWS 20 WLR PQRWY 30 AGRNRELA 40 LAVKPGV 50 VVALR 60
M. marinum 1 MTRSDTLA 10 TKL PWS 20 WLR PQRWY 30 AGRNRELA 40 LAVKPGV 50 VVALR 60
M. ulcerans 1 MTRSDTLA 10 TKL PWS 20 WLR PQRWY 30 AGRNRELA 40 LAVKPGV 50 VVALR 60
Rhodococcusjostii 1 MTRSDTLA 10 TKL PWS 20 WLR PQRWY 30 AGRNRELA 40 LAVKPGV 50 VVALR 60
M. neoaurum 1 MTRSDTLA 10 TKL PWS 20 WLR PQRWY 30 AGRNRELA 40 LAVKPGV 50 VVALR 60
Actinosynemamirum 1 MTRSDTLA 10 TKL PWS 20 WLR PQRWY 30 AGRNRELA 40 LAVKPGV 50 VVALR 60
Actinoplanesmissouriensis 1 MTRSDTLA 10 TKL PWS 20 WLR PQRWY 30 AGRNRELA 40 LAVKPGV 50 VVALR 60
Streptomyceshygroscopicus 1 MTPMAETVTSSGTTGSLLAS 10 DPLLRAWLP 20 PQRWYAGRNRELA 30 AAAEPEGA 40 VVALR 50 EELDL 60 LVLVDVSYTDGS 70 SERV 80 YTDGS 90 AERY 100 AERY 110 AERY 120 AERY 130 AERY 140 AERY
3* ★★
60 QLVVVRWADSPVAGFGEAATIGTALGPQGERIAYDALFDPDAARHLRLVDASATVAD 70 80 90 100 110 120 130 140
70 QVFLVGVDFEPASEYGTKAAGVADD 80 90 100 110 120 130 140
M. tuberculosis 70 QVFLVGVDFEPASEYGTKAAGVADD 80 90 100 110 120 130 140
M. smegmatis 70 QVFLVGVDFEPASEYGTKAAGVADD 80 90 100 110 120 130 140
M. haissiacum 70 QVFLVGVDFEPASEYGTKAAGVADD 80 90 100 110 120 130 140
M. aviumparatuberculosis 70 QVFLVGVDFEPASEYGTKAAGVADD 80 90 100 110 120 130 140
M. marinum 70 QVFLVGVDFEPASEYGTKAAGVADD 80 90 100 110 120 130 140
M. ulcerans 70 QVFLVGVDFEPASEYGTKAAGVADD 80 90 100 110 120 130 140
Rhodococcusjostii 70 QVFLVGVDFEPASEYGTKAAGVADD 80 90 100 110 120 130 140
M. neoaurum 70 QVFLVGVDFEPASEYGTKAAGVADD 80 90 100 110 120 130 140
Actinosynemamirum 70 QVFLVGVDFEPASEYGTKAAGVADD 80 90 100 110 120 130 140
Actinoplanesmissouriensis 70 QVFLVGVDFEPASEYGTKAAGVADD 80 90 100 110 120 130 140
Streptomyceshygroscopicus 70 QVFLVGVDFEPASEYGTKAAGVADD 80 90 100 110 120 130 140
Apo-Mak ★
140 SNTSVILFGKD 150 160 170 180 190 200 210 220
150 SNTSVILFGKD 160 170 180 190 200 210 220
M. tuberculosis 150 SNTSVILFGKD 160 170 180 190 200 210 220
M. smegmatis 150 SNTSVILFGKD 160 170 180 190 200 210 220
M. haissiacum 150 SNTSVILFGKD 160 170 180 190 200 210 220
M. aviumparatuberculosis 150 SNTSVILFGKD 160 170 180 190 200 210 220
M. marinum 150 SNTSVILFGKD 160 170 180 190 200 210 220
M. ulcerans 150 SNTSVILFGKD 160 170 180 190 200 210 220
Rhodococcusjostii 150 SNTSVILFGKD 160 170 180 190 200 210 220
M. neoaurum 150 SNTSVILFGKD 160 170 180 190 200 210 220
Actinosynemamirum 150 SNTSVILFGKD 160 170 180 190 200 210 220
Actinoplanesmissouriensis 150 SNTSVILFGKD 160 170 180 190 200 210 220
Streptomyceshygroscopicus 150 SNTSVILFGKD 160 170 180 190 200 210 220
160 AMLKV 170 180 190 200 210 220
170 SNTSVILFGKD 180 190 200 210 220
180 SNTSVILFGKD 190 200 210 220
190 SNTSVILFGKD 200 210 220
200 RCALGMVTAFAAANSAEGWDMAT 210 220
210 RCALGMVTAFAAANSAEGWDMAT 220
220 RCALGMVTAFAAANSAEGWDMAT 230 240 250 260 270 280 290 300
230 ASAREMFA 240 250 260 270 280 290 300
240 ASAREMFA 250 260 270 280 290 300
M. tuberculosis 230 ASAREMFA 240 250 260 270 280 290 300
M. smegmatis 230 ASAREMFA 240 250 260 270 280 290 300
M. haissiacum 230 ASAREMFA 240 250 260 270 280 290 300
M. aviumparatuberculosis 230 ASAREMFA 240 250 260 270 280 290 300
M. marinum 230 ASAREMFA 240 250 260 270 280 290 300
M. ulcerans 230 ASAREMFA 240 250 260 270 280 290 300
Rhodococcusjostii 230 ASAREMFA 240 250 260 270 280 290 300
M. neoaurum 230 ASAREMFA 240 250 260 270 280 290 300
Actinosynemamirum 230 ASAREMFA 240 250 260 270 280 290 300
Actinoplanesmissouriensis 230 ASAREMFA 240 250 260 270 280 290 300
Streptomyceshygroscopicus 230 ASAREMFA 240 250 260 270 280 290 300
260 STEPFPVDTVLAQLQSAAARSAPELAGRAAAVEERY 270 280 290 300
270 STEPFPVDTVLAQLQSAAARSAPELAGRAAAVEERY 280 290 300
280 STEPFPVDTVLAQLQSAAARSAPELAGRAAAVEERY 290 300
290 STEPFPVDTVLAQLQSAAARSAPELAGRAAAVEERY 300
300 STEPFPVDTVLAQLQSAAARSAPELAGRAAAVEERY 310 320 330 340 350 360 370 380
310 RRLDGRA 320 330 340 350 360 370 380
320 RRLDGRA 330 340 350 360 370 380
330 RRLDGRA 340 350 360 370 380
340 RRLDGRA 350 360 370 380
350 RRLDGRA 360 370 380
360 RRLDGRA 370 380
370 RRLDGRA 380
380 RRLDGRA 390
390 RRLDGRA 400
400 RRLDGRA 410 420 430 440 450
410 RRLDGRA 420 430 440 450
420 RRLDGRA 430 440 450
430 RRLDGRA 440 450
440 RRLDGRA 450
450 RRLDGRA 460
460 RRLDGRA 470
470 RRLDGRA 480
480 RRLDGRA 490
490 RRLDGRA 500
500 RRLDGRA 510
510 RRLDGRA 520
520 RRLDGRA 530
530 RRLDGRA 540
540 RRLDGRA 550
550 RRLDGRA 560
560 RRLDGRA 570
570 RRLDGRA 580
580 RRLDGRA 590
590 RRLDGRA 600
600 RRLDGRA 610
610 RRLDGRA 620
620 RRLDGRA 630
630 RRLDGRA 640
640 RRLDGRA 650
650 RRLDGRA 660
660 RRLDGRA 670
670 RRLDGRA 680
680 RRLDGRA 690
690 RRLDGRA 700
700 RRLDGRA 710
710 RRLDGRA 720
720 RRLDGRA 730
730 RRLDGRA 740
740 RRLDGRA 750
750 RRLDGRA 760
760 RRLDGRA 770
770 RRLDGRA 780
780 RRLDGRA 790
790 RRLDGRA 800
800 RRLDGRA 810
810 RRLDGRA 820
820 RRLDGRA 830
830 RRLDGRA 840
840 RRLDGRA 850
850 RRLDGRA 860
860 RRLDGRA 870
870 RRLDGRA 880
880 RRLDGRA 890
890 RRLDGRA 900
900 RRLDGRA 910
910 RRLDGRA 920
920 RRLDGRA 930
930 RRLDGRA 940
940 RRLDGRA 950
950 RRLDGRA 960
960 RRLDGRA 970
970 RRLDGRA 980
980 RRLDGRA 990
990 RRLDGRA 1000
1000 RRLDGRA 1010
1010 RRLDGRA 1020
1020 RRLDGRA 1030
1030 RRLDGRA 1040
1040 RRLDGRA 1050
1050 RRLDGRA 1060
1060 RRLDGRA 1070
1070 RRLDGRA 1080
1080 RRLDGRA 1090
1090 RRLDGRA 1100
1100 RRLDGRA 1110
1110 RRLDGRA 1120
1120 RRLDGRA 1130
1130 RRLDGRA 1140
1140 RRLDGRA 1150
1150 RRLDGRA 1160
1160 RRLDGRA 1170
1170 RRLDGRA 1180
1180 RRLDGRA 1190
1190 RRLDGRA 1200
1200 RRLDGRA 1210
1210 RRLDGRA 1220
1220 RRLDGRA 1230
1230 RRLDGRA 1240
1240 RRLDGRA 1250
1250 RRLDGRA 1260
1260 RRLDGRA 1270
1270 RRLDGRA 1280
1280 RRLDGRA 1290
1290 RRLDGRA 1300
1300 RRLDGRA 1310
1310 RRLDGRA 1320
1320 RRLDGRA 1330
1330 RRLDGRA 1340
1340 RRLDGRA 1350
1350 RRLDGRA 1360
1360 RRLDGRA 1370
1370 RRLDGRA 1380
1380 RRLDGRA 1390
1390 RRLDGRA 1400
1400 RRLDGRA 1410
1410 RRLDGRA 1420
1420 RRLDGRA 1430
1430 RRLDGRA 1440
1440 RRLDGRA 1450
1450 RRLDGRA 1460
1460 RRLDGRA 1470
1470 RRLDGRA 1480
1480 RRLDGRA 1490
1490 RRLDGRA 1500
1500 RRLDGRA 1510
1510 RRLDGRA 1520
1520 RRLDGRA 1530
1530 RRLDGRA 1540
1540 RRLDGRA 1550
1550 RRLDGRA 1560
1560 RRLDGRA 1570
1570 RRLDGRA 1580
1580 RRLDGRA 1590
1590 RRLDGRA 1600
1600 RRLDGRA 1610
1610 RRLDGRA 1620
1620 RRLDGRA 1630
1630 RRLDGRA 1640
1640 RRLDGRA 1650
1650 RRLDGRA 1660
1660 RRLDGRA 1670
1670 RRLDGRA 1680
1680 RRLDGRA 1690
1690 RRLDGRA 1700
1700 RRLDGRA 1710
1710 RRLDGRA 1720
1720 RRLDGRA 1730
1730 RRLDGRA 1740
1740 RRLDGRA 1750
1750 RRLDGRA 1760
1760 RRLDGRA 1770
1770 RRLDGRA 1780
1780 RRLDGRA 1790
1790 RRLDGRA 1800
1800 RRLDGRA 1810
1810 RRLDGRA 1820
1820 RRLDGRA 1830
1830 RRLDGRA 1840
1840 RRLDGRA 1850
1850 RRLDGRA 1860
1860 RRLDGRA 1870
1870 RRLDGRA 1880
1880 RRLDGRA 1890
1890 RRLDGRA 1900
1900 RRLDGRA 1910
1910 RRLDGRA 1920
1920 RRLDGRA 1930
1930 RRLDGRA 1940
1940 RRLDGRA 1950
1950 RRLDGRA 1960
1960 RRLDGRA 1970
1970 RRLDGRA 1980
1980 RRLDGRA 1990
1990 RRLDGRA 2000
2000 RRLDGRA 2010
2010 RRLDGRA 2020
2020 RRLDGRA 2030
2030 RRLDGRA 2040
2040 RRLDGRA 2050
2050 RRLDGRA 2060
2060 RRLDGRA 2070
2070 RRLDGRA 2080
2080 RRLDGRA 2090
2090 RRLDGRA 2100
2100 RRLDGRA 2110
2110 RRLDGRA 2120
2120 RRLDGRA 2130
2130 RRLDGRA 2140
2140 RRLDGRA 2150
2150 RRLDGRA 2160
2160 RRLDGRA 2170
2170 RRLDGRA 2180
2180 RRLDGRA 2190
2190 RRLDGRA 2200
2200 RRLDGRA 2210
2210 RRLDGRA 2220
2220 RRLDGRA 2230
2230 RRLDGRA 2240
2240 RRLDGRA 2250
2250 RRLDGRA 2260
2260 RRLDGRA 2270
2270 RRLDGRA 2280
2280 RRLDGRA 2290
2290 RRLDGRA 2300
2300 RRLDGRA 2310
2310 RRLDGRA 2320
2320 RRLDGRA 2330
2330 RRLDGRA 2340
2340 RRLDGRA 2350
2350 RRLDGRA 2360
2360 RRLDGRA 2370
2370 RRLDGRA 2380
2380 RRLDGRA 2390
2390 RRLDGRA 2400
2400 RRLDGRA 2410
2410 RRLDGRA 2420
2420 RRLDGRA 2430
2430 RRLDGRA 2440
2440 RRLDGRA 2450
2450 RRLDGRA 2460
2460 RRLDGRA 2470
2470 RRLDGRA 2480
2480 RRLDGRA 2490
2490 RRLDGRA 2500
2500 RRLDGRA 2510
2510 RRLDGRA 2520
2520 RRLDGRA 2530
2530 RRLDGRA 2540
2540 RRLDGRA 2550
2550 RRLDGRA 2560
2560 RRLDGRA 2570
2570 RRLDGRA 2580
2580 RRLDGRA 2590
2590 RRLDGRA 2600
2600 RRLDGRA 2610
2610 RRLDGRA 2620
2620 RRLDGRA 2630
2630 RRLDGRA 2640
2640 RRLDGRA 2650
2650 RRLDGRA 2660
2660 RRLDGRA 2670
2670 RRLDGRA 2680
2680 RRLDGRA 2690
2690 RRLDGRA 2700
2700 RRLDGRA 2710
2710 RRLDGRA 2720
2720 RRLDGRA 2730
2730 RRLDGRA 2740
2740 RRLDGRA 2750
2750 RRLDGRA 2760
2760 RRLDGRA 2770
2770 RRLDGRA 2780
2780 RRLDGRA 2790
2790 RRLDGRA 2800
2800 RRLDGRA 2810
2810 RRLDGRA 2820
2820 RRLDGRA 2830
2830 RRLDGRA 2840
2840 RRLDGRA 2850
2850 RRLDGRA 2860
2860 RRLDGRA 2870
2870 RRLDGRA 2880
2880 RRLDGRA 2890
2890 RRLDGRA 2900
2900 RRLDGRA 2910
2910 RRLDGRA 2920
2920 RRLDGRA 2930
2930 RRLDGRA 2940
2940 RRLDGRA 2950
2950 RRLDGRA 2960
2960 RRLDGRA 2970
2970 RRLDGRA 2980
2980 RRLDGRA 2990
2990 RRLDGRA 3000
3000 RRLDGRA 3010
3010 RRLDGRA 3020
3020 RRLDGRA 3030
3030 RRLDGRA 3040
3040 RRLDGRA 3050
3050 RRLDGRA 3060
3060 RRLDGRA 3070
3070 RRLDGRA 3080
3080 RRLDGRA 3090
3090 RRLDGRA 3100
3100 RRLDGRA 3110
3110 RRLDGRA 3120
3120 RRLDGRA 3130
3130 RRLDGRA 3140
3140 RRLDGRA 3150
3150 RRLDGRA 3160
3160 RRLDGRA 3170
3170 RRLDGRA 3180
3180 RRLDGRA 3190
3190 RRLDGRA 3200
3200 RRLDGRA 3210
3210 RRLDGRA 3220
3220 RRLDGRA 3230
3230 RRLDGRA 3240
3240 RRLDGRA 3250
3250 RRLDGRA 3260
3260 RRLDGRA 3270
3270 RRLDGRA 3280
3280 RRLDGRA 3290
3290 RRLDGRA 3300
3300 RRLDGRA 3310
3310 RRLDGRA 3320
3320 RRLDGRA 3330
3330 RRLDGRA 3340
3340 RRLDGRA 3350
3350 RRLDGRA 3360
3360 RRLDGRA 3370
3370 RRLDGRA 3380
3380 RRLDGRA 3390
3390 RRLDGRA 3400
3400 RRLDGRA 3410
3410 RRLDGRA 3420
3420 RRLDGRA 3430
3430 RRLDGRA 3440
3440 RRLDGRA 3450
3450 RRLDGRA 3460
3460 RRLDGRA 3470
3470 RRLDGRA 3480
3480 RRLDGRA 3490
3490 RRLDGRA 3500
3500 RRLDGRA 3510
3510 RRLDGRA 3520
3520 RRLDGRA 3530
3530 RRLDGRA 3540
3540 RRLDGRA 3550
3550 RRLDGRA 3560
3560 RRLDGRA 3570
3570 RRLDGRA 3580
3580 RRLDGRA 3590
3590 RRLDGRA 3600
3600 RRLDGRA 3610
3610 RRLDGRA 3620
3620 RRLDGRA 3630
3630 RRLDGRA 3640
3640 RRLDGRA 3650
3650 RRLDGRA 3660
3660 RRLDGRA 3670
3670 RRLDGRA 3680
3680 RRLDGRA 3690
3690 RRLDGRA 3700
3700 RRLDGRA 3710
3710 RRLDGRA 3720
3720 RRLDGRA 3730
3730 RRLDGRA 3740
3740 RRLDGRA 3750
3750 RRLDGRA 3760
3760 RRLDGRA 3770
3770 RRLDGRA 3780
3780 RRLDGRA 3790
3790 RRLDGRA 3800
3800 RRLDGRA 3810
3810 RRLDGRA 3820
3820 RRLDGRA 3830
3830 RRLDGRA 3840
3840 RRLDGRA 3850
3850 RRLDGRA 3860
3860 RRLDGRA 3870
3870 RRLDGRA 3880
3880 RRLDGRA 3890
3890 RRLDGRA 3900
3900 RRLDGRA 3910
3910 RRLDGRA 3920
3920 RRLDGRA 3930
3930 RRLDGRA 3940
3940 RRLDGRA 3950
3950 RRLDGRA 3960
3960 RRLDGRA 3970
3970 RRLDGRA 3980
3980 RRLDGRA 3990
3990 RRLDGRA 4000
4000 RRLDGRA 4010
4010 RRLDGRA 4020
4020 RRLDGRA 4030
4030 RRLDGRA 4040
4040 RRLDGRA 4050
4050 RRLDGRA 4060
4060 RRLD

lines above the alignment indicate the domains identified in the three-dimensional structure (blue: cap subdomain; green: intermediate domain; pink: C-terminal domain) and the main structural motifs associated with phosphotransfer activity are highlighted. Residues involved in interactions with the nucleotide are marked below the alignment (stars: residues involved in polar contacts at the interface between the cap and the intermediate domain; yellow circles: residues involved in Van der Waals interactions with the adenine base; green circles: residues involved in water-mediated interactions with the adenine base; red triangles: residues involved in direct hydrogen bonds with the γ -phosphoryl group; green triangles: residues involved in water-mediated polar contacts with the phosphoryl groups; blue triangles: residues directly stabilizing magnesium-coordinating water molecules; magenta triangles: residues involved in magnesium ion coordination). Figure prepared with Aline².



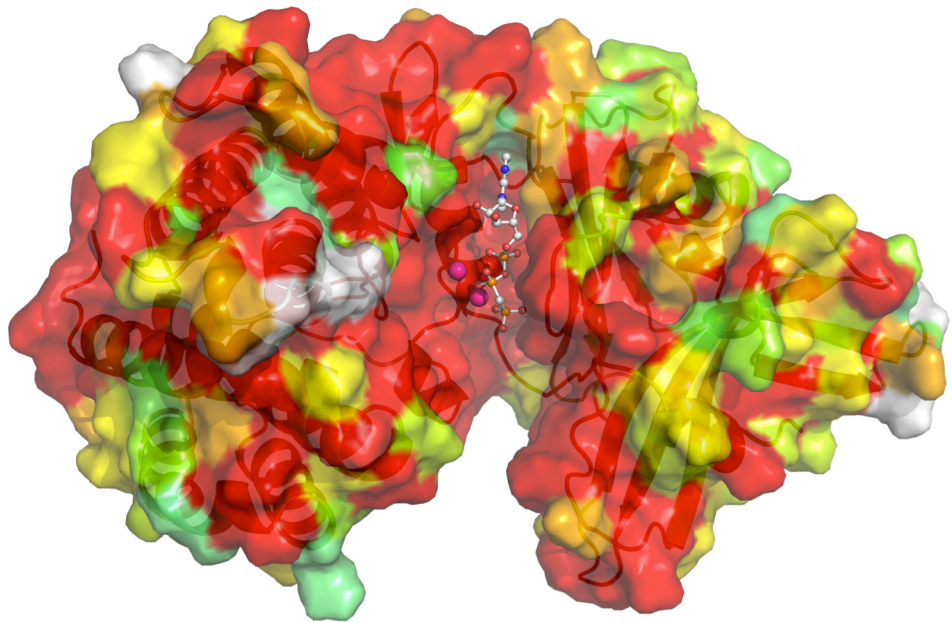
Supplementary Fig. S2 – Location of nucleotide and substrate binding sites in MAK structural homologs

(A) Mak^{Mvan}; (B) MTRK (PDB accession code 2PUN³; (C) aminoglycoside-3'-phosphotransferase-IIa (PDB accession code 1ND4⁴) and (D) 3',5"-aminoglycoside phosphotransferase Type IIIa (PDB accession code 3TM0⁵). Topologically equivalent domains in the different proteins are colored in a similar way, the (adenosine-5'-[(β,γ) -methyleno] triphosphate (AppCp , A and B) and adenosine 5'-[(β,γ) -imido] triphosphate (AppNp, D) analogues bound at the active site cleft are shown as ball-and-stick (A) or as sticks (B, D). The substrate and ligands bound to the substrate binding pocket in these enzymes are shown as spheres with oxygen atoms in red, nitrogen in blue, phosphorus in orange and carbon in yellow. Notice the different orientation of the γ -phosphoryl moiety in Mak^{Mvan} (A) and in MTRK (B) or aminoglycoside phosphotransferase (D).



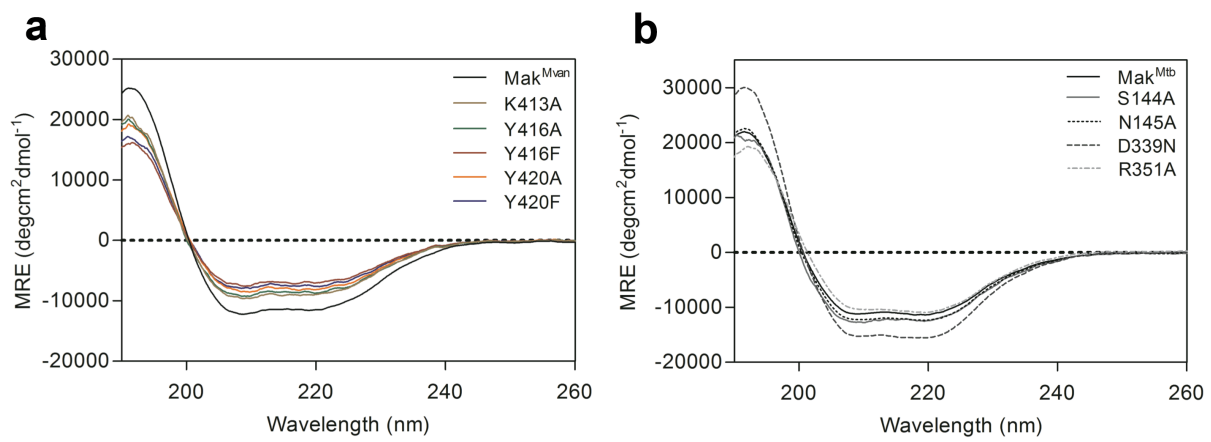
Supplementary Fig. S3 – Nucleotide binding site

(A) Alternate binding mode of AppCp to Mak^{Mvan}. Stereogram of Mak^{Mvan} active site showing the experimental 2Fo-Fc electron density map (blue mesh, contoured at 1σ), and the two modelled conformations of the bound AppCp nucleotide analogue (represented as ball-and-stick with carbon coloured yellow, nitrogen blue, oxygen red, and phosphorous orange). (B) The binding mode of ATP to Mak^{Mvan}. Stereogram of Mak^{Mvan} active site (the Mak^{Mvan}:ATP complex [white cartoon] is shown superposed to the Mak^{Mvan}:AppCp complex [pink cartoon]) showing the experimental 2Fo-Fc electron density map (blue mesh, contoured at 0.7σ) for the bound ligand (sticks, atoms color-coded as in (A)). The two identified conformations of the AppCp in the Mak^{Mvan}:AppCp complex are shown as lines, for comparison purposes. No electron density is found for the two terminal phosphates, which were removed from the final model.



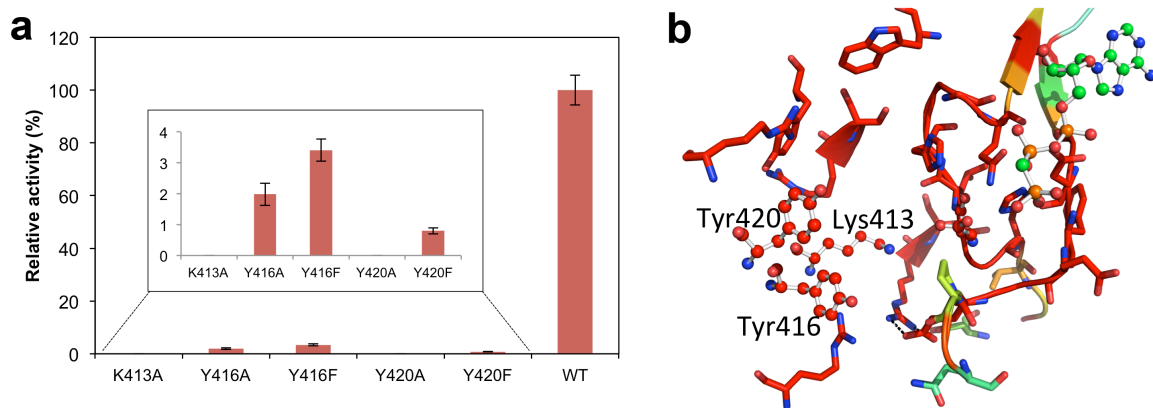
Supplementary Fig. S4. Conservation of key residues in *M.tuberculosis* maltokinase

Surface representation of Mak^{Mvan} coloured according to residue conservation between the maltokinases from *M. vanbaalenii* and *M. tuberculosis* (red: identical residues, orange to blue: scale of decreasing conservation of amino acid properties; white: dissimilar residues). Figure prepared with PyMOL (<http://www.pymol.org>).



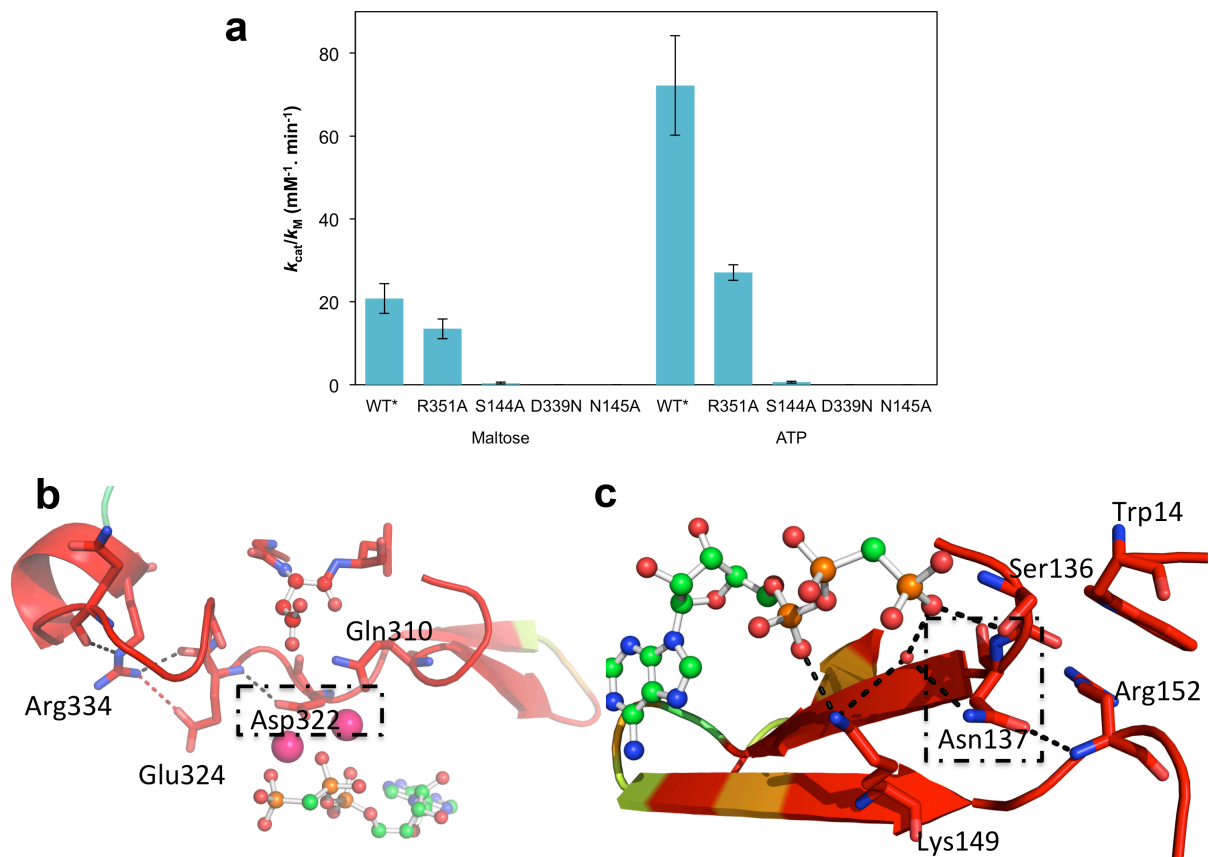
Supplementary Fig. S5 – Far UV CD spectra of Mak variants

CD spectra of wild-type Mak^{Mvan}(A) and Mak^{Mtb} (B) and of their point mutants, revealing no significant differences in secondary structure content.



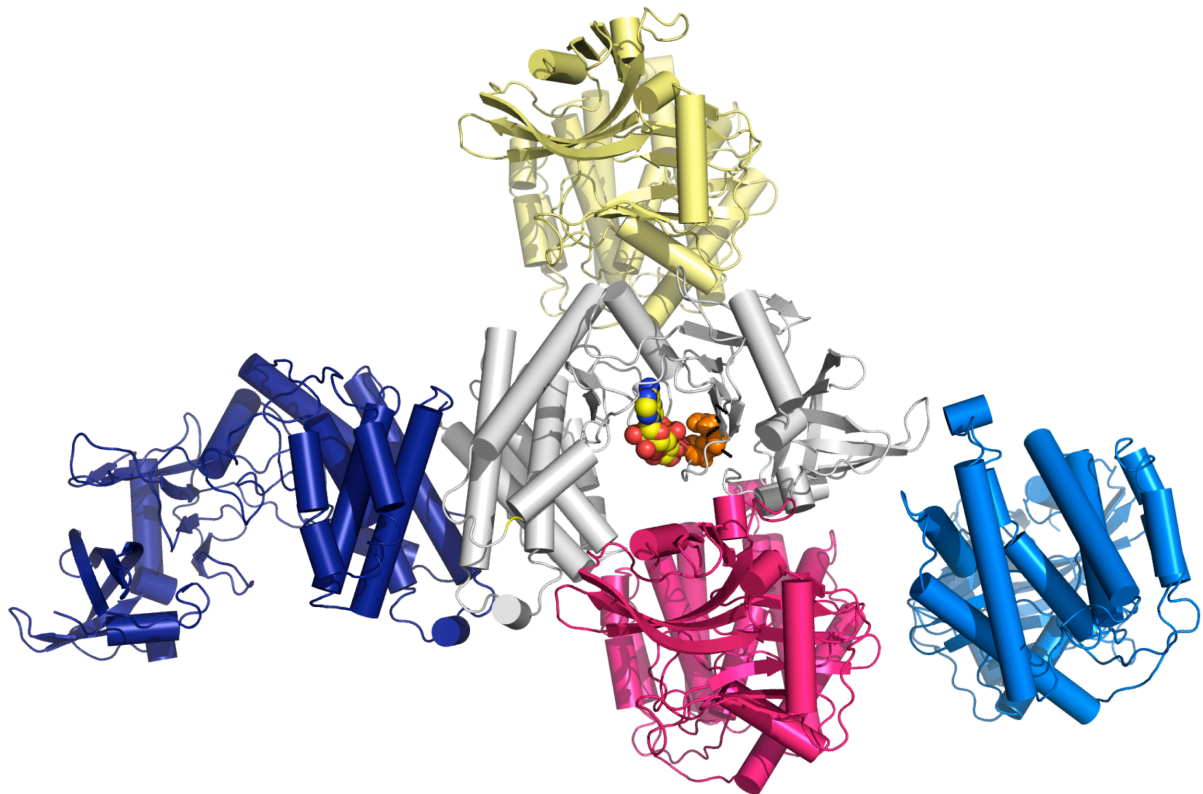
Supplementary Fig. S6 - Mutational analysis of Mak^{Mvan} maltose binding site

(A) Analysis of the effect of point mutations in key residues for Mak^{Mvan} catalytic activity. (B) Detailed view of the putative maltose-binding cavity (as in Fig. 6B) highlighting the residues selected for mutational analysis as ball-and-stick representation (oxygen atoms in red, nitrogen in blue, phosphorus in orange and carbon coloured according to sequence conservation as in Supplementary Fig. S4). AppCp is shown as ball-and-stick with carbons in green. Panel B prepared with PyMOL (<http://www.pymol.org>).



Supplementary Fig. S7 – Mutational analysis of *M. tuberculosis* Mak P-loop residues and DFE motif

(A) Analysis of the effect of point mutations in key residues for Mak^{Mtb} catalytic efficiency (k_{cat}/k_M). The mutated residues Arg351, Ser144, Asp339, and Asn145 are conserved in Mak^{Mvan} (Arg334, Ser136, Asp322, and Asn137, respectively) (B-C). Detailed view of key interactions in the catalytic loop (B) and in the P-loop (C) of Mak^{Mvan}, highlighting the residues selected for mutational analysis (dashed rectangles). Selected residues are shown as sticks and Asp305 and nucleotide as ball-and-stick with oxygen atoms in red, nitrogen in blue, phosphorus in orange and carbon in green (nucleotide) or according to sequence conservation (protein, colours as in Supplementary Fig. S4). Hydrogen bonds are represented as dashed black lines and magnesium ions as magenta spheres. Panels B and C prepared with PyMOL (<http://www.pymol.org>).



Supplementary Fig. S8 – Symmetry neighbours in Mak^{Mvan} crystals

Mak^{Mvan} is represented as a white cartoon and the nucleotide (two modelled conformations) as spheres. The P-loop residues Ser136 and Asn137 are represented as orange spheres. The neighbouring molecules in the crystal involved in significant crystal contacts are shown as cartoon representations in different colours. The largest crystal contact interface involves the C-terminal helical domain (dark blue; crystal contact buries 6% of the total solvent-accessible area), followed by a crystal contact affecting the tips of the central cleft, particularly the N-terminal domain and a large portion of the C-terminal domain (pink; buries 5% of total solvent-accessible area). The crystal contacts mediated by the external face of the intermediate (yellow) and N-terminal subdomains (marine blue) are less extensive, burying only 3% and 2% of total solvent-accessible area, respectively.

Supplementary Table S1: Mak^{Mvan} structural neighbours

Full length protein				
Protein name	PDB entry	Z-score / r.m.s.d. (Å)	Number of aligned residues	Amino acid sequence identity* (%)
Methylthioribose kinase	2pul ³	19.0 / 3.7	272	10
Choline/ethanolamine kinase family protein	3dxq	18.6 / 4.1	258	13
Homoserine kinase	2ppq	18.4 / 3.3	261	15
YTAA protein	2q83 ⁶	18.1 / 3.3	271	16
Spectinomycin phosphotransferase	3i1a ⁷	16.9 / 3.6	259	12
Putative aminoglycoside phosphotransferase	3csv	16.2 / 3.6	255	13
N-terminal Cap domain				
Multicystatin	2w9p ⁸	4.3 / 2.6	59	14
Serine/threonine protein kinase GCN2	1zy4 ⁹	4.2 / 3.3	60	7
Putative NTF2-Like Transpeptidase	3k7c	4.1 / 2.7	61	10

*Structure-based sequence alignment, as calculated by Dali server

(http://ekhidna.biocenter.helsinki.fi/dali_server/start)¹⁰.

Supplementary Table S2 – Summary of parameters for pockets identified in free Mak^{Mvan}

Pocket number	Total SASA (Å ²)	Polar SASA (Å ²)	Apolar SASA (Å ²)	Volume (Å ³)	Proportion of polar atoms (%)
1	719	352	357	1728	36.6
2	591	345	246	1572	53.3
3	513	221	292	1071	45.5
4	137	48	89	209	54.2
5	377	200	177	724	46.1

SASA – Solvent-accessible surface area

Supplementary Table S3 – Oligonucleotides used as PCR primers

Code	Name	Sequence (5'-3')
MakF	MakF	ATTGATCAAC <u>ATAT</u> GACGCTGGCATTGGCGATTG
MakR	MakR	AT <u>CAAG</u> CTTGC <u>CCAGG</u> ATGAGGCTGATCGATC
A	WT_NdeF	CTTA <u>CATAT</u> GACTCGGT <u>CGG</u> ACACGC
B1	S144A_F	GACGCCGAACAG <u>GCC</u> AACACCAGTG
C1	S144A_R	CACTGGT <u>GTT</u> <u>GCG</u> CTGTT <u>CGG</u> CGTC
D	WT_HindR	ATTA <u>AGCTT</u> GCTAGCGGT <u>CAGG</u> CGGG
B2	N145A_F	GACGCCGAACAG <u>GAGC</u> <u>GCC</u> ACCAGTG
C2	N145A_R	CACTGGT <u>GGC</u> GCTCTGTT <u>CGG</u> CGTC
	Mak K413A_F	GCCTACGAG <u>CTCGAC</u> <u>GCG</u> CGGGTGTACGAAGC
	Mak K413A_R	GCTTC <u>GTACACC</u> <u>GCG</u> GTCGAG <u>CTCGT</u> AGGC
	Mak Y416A_F	CTCGACAAGG <u>CGGTG</u> <u>GCC</u> GAAGCCGCTTACGA
	Mak Y416A_R	TCGTAAG <u>CGG</u> CTTC <u>GGC</u> CACCGC <u>TTGTC</u> GAG
	Mak Y416F_F	CTCGACAAGG <u>CGGTG</u> <u>TTC</u> GAAGCCGCTTA
	Mak Y416F_R	TAAG <u>CGG</u> CTTC <u>GAA</u> CACCGC <u>TTGTC</u> GAG
	Mak Y420A_F	GGTGTACG <u>AAGCCG</u> <u>GCC</u> GAGGCC <u>CGTT</u> CC
	Mak Y420A_R	GGAA <u>ACGGG</u> C <u>CTC</u> <u>GGC</u> AG <u>CGG</u> CTT <u>CGT</u> ACACC
	Mak Y420F_F	TGTACG <u>AAGCCG</u> <u>TTC</u> GAGGCC <u>CGTT</u> CC
	Mak Y420F_R	GAA <u>ACGGG</u> C <u>CTC</u> <u>GAA</u> AG <u>CGG</u> CTT <u>CGT</u> A

NdeI and HindIII restriction sites are underlined. Mutated codons are boxed.

- 1 Whitmore, L. & Wallace, B. A. DICHROWEB, an online server for protein secondary structure analyses from circular dichroism spectroscopic data. *Nucleic Acids Res* **32**, W668-673 (2004).
- 2 Bond, C. S. & Schuttelkopf, A. W. ALINE: a WYSIWYG protein-sequence alignment editor for publication-quality alignments. *Acta Crystallogr D Biol Crystallogr* **65**, 510-512 (2009).
- 3 Ku, S. Y. *et al.* Structures of 5-methylthioribose kinase reveal substrate specificity and unusual mode of nucleotide binding. *J Biol Chem* **282**, 22195-22206 (2007).
- 4 Kannan, N., Taylor, S. S., Zhai, Y., Venter, J. C. & Manning, G. Structural and functional diversity of the microbial kinome. *PLoS Biol* **5**, e17 (2007).
- 5 Nobre, A., Alarico, S., Maranha, A., Mendes, V. & Empadinhas, N. The molecular biology of mycobacterial trehalose in the quest for advanced tuberculosis therapies. *Microbiology* **160**, 1547-1570 (2014).
- 6 Scheeff, E. D. *et al.* Genomics, evolution, and crystal structure of a new family of bacterial spore kinases. *Proteins* **78**, 1470-1482 (2010).
- 7 Fong, D. H., Lemke, C. T., Hwang, J., Xiong, B. & Berghuis, A. M. Structure of the antibiotic resistance factor spectinomycin phosphotransferase from *Legionella pneumophila*. *J Biol Chem* **285**, 9545-9555 (2010).
- 8 Nissen, M. S. *et al.* Characterization of *Solanum tuberosum* multicystatin and its structural comparison with other cystatins. *Plant Cell* **21**, 861-875 (2009).
- 9 Padyana, A. K., Qiu, H., Roll-Mecak, A., Hinnebusch, A. G. & Burley, S. K. Structural basis for autoinhibition and mutational activation of eukaryotic initiation factor 2alpha protein kinase GCN2. *J Biol Chem* **280**, 29289-29299 (2005).
- 10 Holm, L. & Rosenstrom, P. Dali server: conservation mapping in 3D. *Nucleic Acids Res* **38**, W545-549 (2010).